https://doi.org/10.48048/tis.2023.4058

On the Optical Properties of the $Cu_2ZnSn[S_{1-x}Se_x]_4$ System in the IR Range

Nematov Dilshod[1,2,*], Kholmurodov Kholmirzo[2,3], Stanchik Aliona[4], Fayzullaev Kahramon[5], Gnatovskaya Viktoriya[6] and Kudzoev Tamerlan[7]

[1]Physical-Technical Institute of National Academy of Sciences of Tajikistan, Dushanbe 734042, Tajikistan
[2]Joint Institute for Nuclear Research, Dubna, Moscow Region 141980, Russia
[3]Dubna State University, Dubna, Moscow Region 141980, Russia
[4]Scientific and Practical Materials Research Center, National Academy of Sciences of Belarus, Minsk 220072, Belarus
[5]Institute of Semiconductor Physics and Microelectronics, Tashkent 100057, Uzbekistan
[6]Institute of Physical Organic Chemistry and Coal Chemistry, Donetsk 02160, Ukraine
[7]Kosta Levanovich Khetagurov NOSU, Ossetia 362025, Russia

([*]Corresponding author's e-mail: dilnem@mail.ru)

Received: 8 May 2022, Revised: 4 June 2022, Accepted: 14 June 2022, Published: 29 November 2022

Abstract

Following the recent classification by the European Commission of some elements as critical raw materials (CRM), there is an increasing interest in the development of CRM-free thin film photovoltaic (PV) technologies, including kesterite materials. Moreover, starting with the performance breakthrough reported by IBM in 2010, the efficiency of kesterite-based solar cells steadily progressed in the following years achieving. Therefore, in recent years, there has been a significant research effort to develop kesterite-based devices. However, despite the large number of theoretical and experimental works, many aspects of the problem have not yet been fully studied. Therefore, the issues considered in the article, especially the behavior of the absorption and photoconductivity spectra of the $Cu_2ZnSn[S_{1-x}Se_x]_4$ system, depending on the S/Se ratio, are extremely important and, at the same time, one of the topical and poorly studied problems. In this work, using quantum-chemical calculations in the framework of density functional theory (DFT), we study the optical properties of semiconductor nanocrystals of kesterite Cu_2ZnSnS_4 doped with Se. Using the WIEN2k package, the concentration dependences of the optical characteristics of nanocrystals of the $Cu_2ZnSn[S_{1-x}Se_x]_4$ system (x = 0.00, 0.25, 0.50, 0.75 and 1.00) were calculated. It is shown that doping with Se at the S position leads to a noticeable improvement in the photoabsorbing properties of these nanocrystals, as well as their photoconductivity in the IR range. The calculated absorption and extinction spectra, as well as the refractive indices and permittivity of the materials under study, are compared with experimental data known from the literature. The data obtained will significantly enrich the existing knowledge about the materials under study and will contribute to the expansion of the field of application of these compounds in optoelectronic devices.

Keywords: Optical materials, Thin film solar cells, Kesterites, CZTSSe, Band gap, Optical properties, Photovoltaic Applications, Density functional theory, mBJ potential

Introduction

Since the beginning of the 21st century, environmental pollution and lack of energy resources have become an increasingly acute problem related to the survival of mankind and development of science. Therefore, increasing the share of renewable energy consumption and protecting the environment are gradually attracting more and more attention around the world. In order to keep the sustainable development of life, governments, research institutes and enterprises are working on the problems caused by the lack of energy resources. It is well known that the best way to solve environmental problems is the use of renewable energy sources and the use of new energy-efficient materials for this purpose [1]. Solar energy is considered to be the most economical and efficient renewable energy source available. It is inexhaustible and "environmentally friendly", does not produce waste and additional heat load on the environment when used [1,2].

Recently, photovoltaic (PV) systems have received a lot of attention due to their advantage over other renewable energy sources due to the ability to directly convert solar energy into electricity, avoiding system wear caused by mechanical movement (since photovoltaic systems do not necessarily contain moving parts), etc. Therefore, solar power plants can operate continuously without maintenance for longer than devices using other power generation technologies. On the other hand, the theoretical conversion efficiency of photovoltaic systems is relatively higher than that of other generators [2].

Currently, 3 thin-film materials are widely used in the industrial production of solar cells: amorphous silicon (a-Si), cadmium telluride (CdTe) and copper-indium-gallium selenide/sulfide $CuIn_xGa_{1-x}S(Se)_2$ (CIGS), among which CIGS has achieved the highest efficiency (20.8 % in laboratory devices) and can compete with polycrystalline silicon [3,4]. Thin-film silicon-based solar cells have been relatively underdeveloped due to low efficiency and instability as a result of the Stabler-Vronsky effect [2]. The other 2 thin-film technologies suffer from serious manufacturing toxicity issues, soaring material costs and/or low natural abundance of raw materials, which are predicted to severely limit the production, mass deployment and economic sustainability of these solar cells [5-12]. Indium (In) is a rare element and may run out in the next 10 - 20 years, while its price has been rising rapidly in recent years [12]. The use of toxic cadmium (Cd) has hindered the mass production and adoption of CdTe solar cells due to environmental aspect concerns [13]. Thus, intensive research is needed to develop alternative thin-film solar-absorbing materials, including naturally occurring, inexpensive and non-toxic elements that can be incorporated into high-performance devices, be economically competitive with traditional energy sources. Cu_2SnS_3 (CTS), Cu_2ZnSnS_4 (CZTS) and $Cu_2ZnSnSe_4$ (CZTSe) compounds are being investigated as a potential alternative to the widely used CdTe and CIGS ($CuInGaSe_2$) solar absorbers [14]. On the other hand, it will be very interesting to synthesize and study their shifted structure, since these semiconductors attract attention as photon-absorbing layers of thin-film solar cells due to their direct band gap of 1.0 - 1.5 eV, high optical absorption coefficient ($> 10^4$ cm^{-1}) and p-type conductivity [15-18]. In addition, they consist of cheap and environmentally friendly elements. The reserves of copper (Cu), zinc (Zn), tin (Sn) and sulfur (S) in the earth's crust are 68, 79, 2.2 and 420 ppm, respectively, compared to 0.16 ppm (In), 0.15 ppm (Cd) and 0.001 ppm (Te) [19]. Calculations on the photon balance of Shockley-Keisser estimated the theoretical conversion efficiency of CZTS single-junction solar cells at 32.2 % [20]. Over the past few years, the efficiency of solar cells based on CTS and CZTS has reached a record value of 4.63 and 9.2 %, respectively [21,22].

Every year, the number of publications devoted to these materials and the number of scientific groups that use various techniques to create and study thin layers of these materials is increasing. However, the study of the fundamental properties of these compounds, especially their optical and elastic properties, remains at a rather low level, which hinders a further increase in the efficiency of structures based on them.

It is important to note that the modeling of physical phenomena has long been an important area of interdisciplinary research, and quantum-chemical studies of nanoscale structures based on semiconductor materials, in particular kesterites, are of great interest in connection with the creation of reliable optoelectronic devices based on them. In contrast to a bulk material, in which an indirect band gap prevents effective photon generation, kesterite nanocrystals exhibit relatively intense radiation [23] in the red and near infrared (IR) ranges. As mentioned above, a great advantage of using nanocrystals and thin films as key elements in the creation of radiation sources is the ability to control their electron-optical properties, which can be done, for example, by changing the material matrix, the size of nanoclusters, introducing impurities, atoms, etc. In this regard, much attention is currently paid to the theoretical and experimental study of the optoelectronic structure of kesterite nanocrystals. One of the most powerful theoretical approaches to studying the band structure and optical properties of not only nanocrystals but also bulk systems is the density functional theory (DFT) method. On the other hand, this method is currently one of the most universal first-principles (ab initio) methods for calculating the electronic structure, optical properties, elasticity and various other characteristics of multiparticle systems and is used in solid state physics and quantum chemistry. The description of a multielectron system within the framework of DFT is carried out not with the help of the wave function, which would cause a very large dimension of the problem (at least equal to 3N values of the coordinates of N particles), but with the help of the electron density function, a function of only 3 spatial coordinates, which leads to a significant simplification tasks. It turns out that the most important properties of a system of interacting particles can be expressed using the electron density functional, in particular, according to the Hohenberg-Kohn theorems [24,25], which provide the theoretical basis for the DFT method, such a functional is the energy of the ground state of the system.

In condensed matter physics, especially for accurate DFT calculations of the structural, electronic, and optical properties of nanomaterials, software packages based on the linearized augmented plane wave method are very effective. One such software package is WIEN2k [26], which has been widely implemented in recent years for high-precision modeling of the properties of solid materials using distributed multiprocessor computing based on technologies such as MPI and CUDA that support standard parallel programming technologies.

In this work, using the WIEN2k package, we calculated the optical properties of both pure and undoped kesterites of the Cu_2ZnSnS_4 and $Cu_2ZnSnSe_4$ systems and their displaced structures ($Cu_2ZnSn[S/Se]_4$) depending on the ratio of sulfur and selenium. In a recent work, the geometry and electronic band structure of the studied materials were studied using ab initio mBJ-calculations [27]. However, the optical properties of these nanocrystals, especially with the use of the mBJ exchange-correlation functional, have not been previously studied.

Crystal structure and computation methods

Ab initio quantum chemical calculations within the framework of DFT were performed on the basis of our optimized orthorhombic lattices of pure and selenium-doped Cu_2ZnSnS_4 from a previous work [27], for which the electronic properties were also studied taking into account spin-polarized and spin-orbital effects. Thus, at the first stage, the structures were optimized in order to determine the equilibrium positions of atoms from the forces acting on the atoms. Calculations of the geometric structure and optoelectronic properties of Cu_2ZnSnS_4 doped with selenium after geometry optimization were performed using a full-potential plane wave packet and a local orbit WIEN2k, where the exchange-correlation effects were estimated by the modified TB-mBJ potential [28]. Numerous works state that this exchange-correlation functional gives an experimentally comparable estimate of the band gap and parameters of optical properties [29-34] compared to other known approximations. The scheme and stages of mBJ calculations for evaluating the electronic and optical properties of materials are shown in [35]. The optimal plane wave cutoff value K_{max} was chosen to be 6.0 $Ry^{1/2}$ after performing convergence tests. A uniform 1×1×1 k-point grid was used for all calculations. The Kohn-Sham equations were solved on the basis of LAPW. For calculations of optical properties, the muffin-tin radii for $Cu_2ZnSn[S_{1-x}Se_x]_4$ nanocrystals (x = 0.00, 0.25, 0.50, 0.75 and 1.00) were 2.31, 2.39, 2.50, 1.96 and 2.20 a.u. for Cu, Zn, Sn, S and Se, respectively. However, the crystal lattices of the optimized structures are shown in **Figure 1**, for which a change in the interplanar distance is visible, leading to changes in intensity, the ability to absorb and reflect the light incident on it, after selenium doping.

All computer calculations were performed on a high-performance computing cluster equipped with 1 computing node with 1 physical processor Intel Core I9-9960X CPU 3.10 G (16 cores at 3.0 GHz) and 32 GB of RAM.

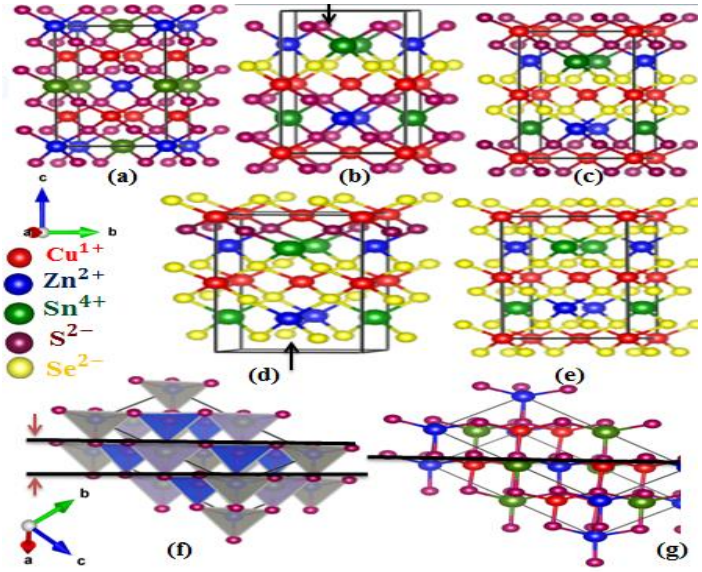

Figure 1 Models of crystal structures: (a) Cu_2ZnSnS_4, (b) Cu_2ZnSnS_3Se, (c) $Cu_2ZnSnS_2Se_2$, (d) $Cu_2ZnSnSSe_3$, (e) $Cu_2ZnSnSe_4$, (f) and (g) show the change in the interplanar spacing in the $Cu_2ZnSnS_{4-x}Se_x$ system.

Calculation of optical properties

All solid materials have the ability to absorb, transmit and reflect processes that can be quantified and modeled at the macroscopic and microscopic levels. At the microscopic (quantum-mechanical) level in bulk nanostructures, the complex dielectric function is strongly related to the band structure. The optical characteristics of kesterite are calculated directly from the complex dielectric function ε(ω), which contains the real $\varepsilon_1(\omega)$ and imaginary $\varepsilon_2(\omega)$ parts as frequency dependent functions. The components of the imaginary part of the permittivity tensor $\varepsilon_2(\omega)$ are calculated from the expression [36]:

$$\varepsilon_2^{ij}(\omega) = \frac{4\Pi^2 e^2}{\Omega}\frac{1}{q^2}\lim_{q\to 0}\sum_{c,\vartheta,k} 2\omega_k \delta(\epsilon_{ck} - \epsilon_{\vartheta k} - \omega) \times \langle u_{ck+e_\alpha q}|u_{ck}\rangle\langle u_{ck+e_\alpha q}|u_{\vartheta k}\rangle^* \quad (1)$$

To estimate the real part of the dielectric function $\varepsilon_1(\omega)$ through the function $\varepsilon_2(\omega)$, the Kramers-Kronig dispersion equation is used:

$$\varepsilon_1^{ij}(\omega) = 1 + \frac{2}{\Pi}\mathrm{P}\int_0^\infty \lim_{q\to 0}\frac{\varepsilon_2^{ij}(\omega')\omega'}{\omega'^2 - \omega^2 + in}\, d\omega', \quad (2)$$

where P represents the principal value of the integral.

Given expressions 1 and 2, all other optical characteristics, including the absorption coefficient α (ω), the real part of the refractive index n(ω), the imaginary part of the extinction coefficient k(ω), the energy loss spectrum L (ω) and the photoconductivity spectra σ (ω), can be obtained using the expressions:

$$\mathrm{L}(\omega) = \frac{\varepsilon_2(\omega)}{\varepsilon_1^2(\omega) + \varepsilon_2^2(\omega)} \quad (3)$$

$$\mathrm{n}(\omega) = \left|\frac{\sqrt{\varepsilon_1^2 + \varepsilon_2^2} + \varepsilon_1}{2}\right|^{\frac{1}{2}} \quad (4)$$

$$\mathrm{k}(\omega) = \left|\frac{\sqrt{\varepsilon_1^2 + \varepsilon_2^2} - \varepsilon_1}{2}\right|^{\frac{1}{2}} \quad (5)$$

$$\alpha(\omega) = \frac{2\omega \mathrm{k}(\omega)}{\mathrm{c}} = \frac{\varepsilon_2(\omega)\omega}{\mathrm{n}(\omega)\mathrm{c}} \quad (6)$$

$$\sigma(\omega) = \sigma_1(\omega) + \mathrm{i}\sigma_2(\omega) = -\mathrm{i}\frac{\omega}{4\pi}[\varepsilon(\omega) - 1] = \frac{\varepsilon_2(\omega)\omega}{4\pi} + \mathrm{i}\frac{1 - \varepsilon_1(\omega)\omega}{4\pi}, \quad (7)$$

where $\varepsilon(\omega) = \varepsilon_1(\omega) + i\varepsilon_2(\omega)$ – a frequency-dependent complex dielectric function.

Thus, the dielectric function can serve as the main bridge between the electronic structure of a solid and a microphysical transition.

Results and discussion

The optical properties of nanocrystals of the $Cu_2ZnSn[S_{1-x}Se_x]_4$ (x = 0.00, 0.25, 0.50, 0.75 and 1.00) system were studied and calculated after obtaining the relaxed structures of these materials. Geometry optimization was carried out due to the relaxation of all positions of atoms in the cell and the shape of the cell, which is inevitable for describing the structural behavior of materials. The optimized structural parameters of Se-doped Cu_2ZnSnS_4 ($Cu_2ZnSn(S_{1-x}Se_x)_4$ family system) are summarized in **Table 1**.

Table 1 Comparison of our calculation results with experimental ones (XRD, PDP and HR-TEM methods) for $Cu_2ZnSn[S_{1-x}Se_x]_4$ system depending on the ratio of S/Se.

$Cu_2ZnSn(S_{1-x}Se_x)_4$ System	Lattice parameters				Error in volume, %
	a = *b*, *c*, Å		*V*, Å^3		
	This work	Experiment	This work	Experiment	
x = 0.00	5.47, 10.72	5.41[a], 10.88[a] 5.46[a], 10.90[a] 5.44[b], 10.87[b]	322.72	320.50[a] 323.75[a] 321.68[b]	0.69 0.31 0.32
x = 0.25	5.56, 10.78	-	333.77	-	-
x = 0.50	5.63, 10.88	-	345.21	-	-
x = 0.75	5.75, 11.01	-	364.24	-	-
x = 1	5.75, 11.08	5.70[b], 11.43[b] 5.70[c], 11.38[c] 5.69[d], 11.32[d]	367.49	370.38[b] 369.73[c] 366.49[d]	0.78 0.60 0.27

[a][37], [b][38], [c][39] and [d][40]

For the studied nanocrystals of the $Cu_2ZnSn[S_{1-x}Se_x]_4$ family system, the permittivity tensors were first determined in accordance with the directions of the initial structure. Further, using the Kramers-Kronig relations and Eqs. (3) - (9), from the spectral dependence of the dielectric permittivity tensor, absorption spectra α (ω), refractive indices n(ω), extinction coefficient k(ω), energy loss spectrum L (ω) and optical conductivity σ(ω) along the crystallographic axis a (along the direction). **Figures 2** and **3** show the calculated real $\varepsilon_1(\omega)$ and imaginary $\varepsilon_2(\omega)$ parts of the dielectric permittivity of kesterites of the $Cu_2ZnSn[S_{1-x}Se_x]_4$ system depending on the energy of incident IR light photons according to mBJ calculations.

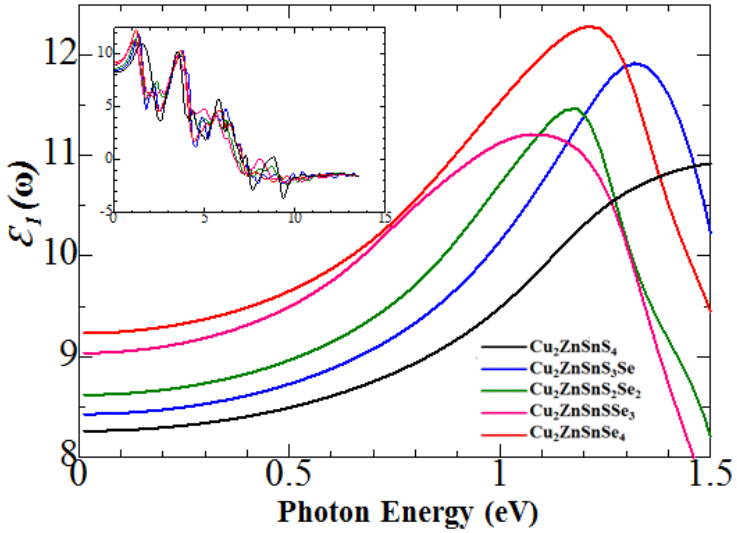

Figure 2 Real part of the dielectric function for kesterites of the $Cu_2ZnSn[S_{1-x}Se_x]_4$ system, calculated using the mBJ approximations (inset: $\varepsilon_1(\omega)$ in the range from 0 to 14 eV).

According to the inset in **Figure 2**, upon absorption of high-energy short-wavelength photons, all these displaced kesteites exhibit metallic behavior. The negative value of ε_1 indicates the metallic nature of these materials. In other words, the metallicity of materials can be investigated and evaluated from the real part of the permittivity. According to **Figure 2** shows that $\varepsilon_1(\omega)$ increases upon passing from sulfur to selenium. This is indicated by the inverse dependence of the band gap on $\varepsilon_1(\omega)$.

In what follows, we will focus on the imaginary part of the complex permittivity, since $\varepsilon_2(\omega)$ is fundamental for determining other spectral characteristics of a solid.

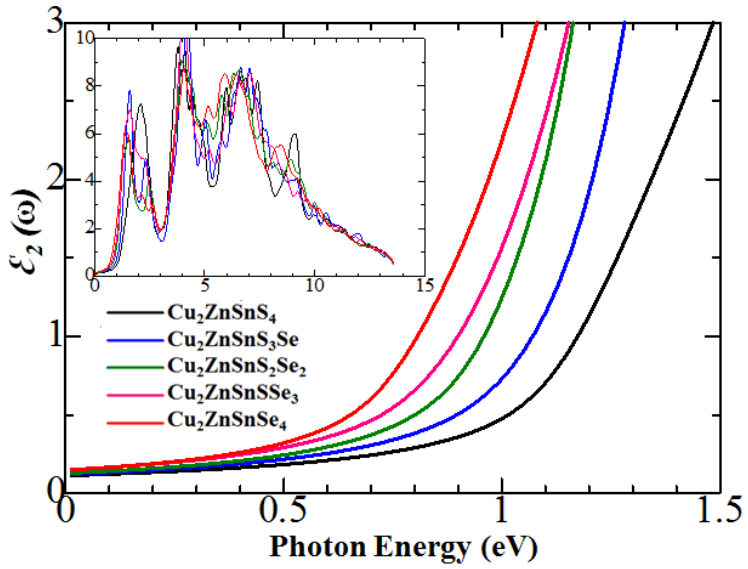

Figure 3 Imaginary part of the dielectric function for kesterites of the $Cu_2ZnSn[S_{1-x}Se_x]_4$ system, calculated using the mBJ approximations (inset: $\varepsilon_2(\omega)$ in the range from 0 to 14 eV).

The $\varepsilon_2(\omega)$ spectrum of nanocrystals of the $Cu_2ZnSn[S_{1-x}Se_x]_4$ system is dominated by three peaks located at 1.9, 4.7 and 7.2 eV, respectively. These peaks can explain the results of calculations of the total density of electronic states published in our previous work [27], in which the reflectivity of these nanocrystals was also estimated. In this case, the peak at 1.9 eV, determined from calculations of the total and partial densities of electronic states, represents transitions from the Cu-3d/S-3p states to the Sn-5s/S-3p band. The peak at 4.7 eV refers to transitions from the Cu-3d/S-3p states to the Sn-5p/S-3p states or transitions from the hybridization of the Cu-3d, Sn-5p and S-3p states to the antibonding Sn-5s/C-3p states. The peak at 7.2 eV is associated with transitions from the hybridization of the Cu-3d, Sn-5p and S-3p states to the antibonding Sn-5p/S-3p states. The $\varepsilon_2(\omega)$ spectrum of $Cu_2ZnSnSe_4$ exhibits a shift of the peaks towards low energies due to a slightly smaller band gap than that of Cu_2ZnSnS_4.

All other optical properties were calculated from $\varepsilon_1(\omega)$ or $\varepsilon_2(\omega)$. **Figures 4 - 7**, respectively show the calculated spectra of refractive indices n(ω), extinction coefficients k(ω), absorption coefficients α (ω) and energy losses L(ω), real and imaginary parts of photoconductivity σ(ω).

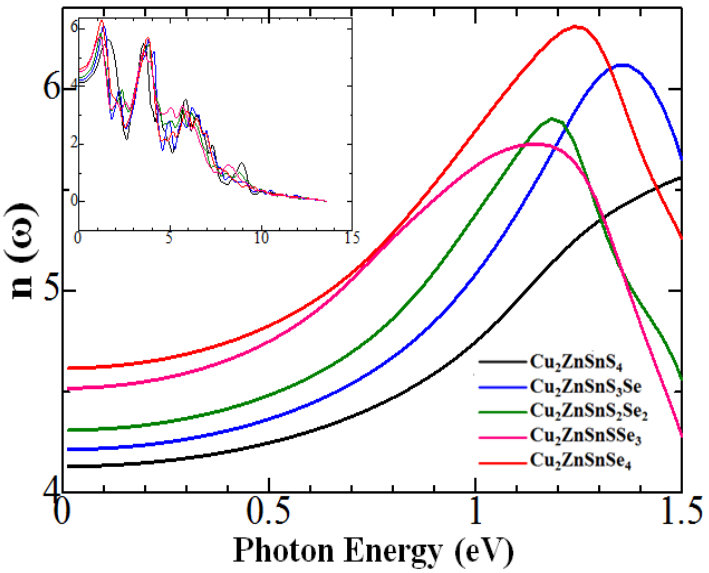

Figure 4 Calculated spectra of dependences of the refractive index of nanocrystals of the $Cu_2ZnSn[S_{1-x}Se_x]_4$ system on the photon energy (insert: n(ω) in the range from 0 to 14 eV).

The calculated refractive index curves for nanocrystals of the $Cu_2ZnSn[S_{1-x}Se_x]_4$ system look similar to the corresponding spectra $\varepsilon_1(\omega)$. These structures have a wide spectrum for n(0) in a wide energy range. In the region of low photon energies, the refractive index corresponds to the band gap. The maximum values of n(ω) are in the energy range 1.8 - 4.6 eV, and then the curves tend to 0 at higher energies.

Usually, when light propagates in a medium, dissipation (weakening) of a light beam, the cause of which is the combined action of the processes of absorption and scattering of light during its propagation in a substance [41,42]. This is an optical property of a material related to the refractive index of the material. The measure of light attenuation is the light extinction coefficient (k). Positive value of k shows that the absorption is going to be take place, while k = 0 shows that the light travels straight through the material. However, if scattering plays no role compared to absorption, then the extinction coefficient becomes the same as the absorption coefficient. On the other hand, the extinction coefficient of materials means how actively a substance absorbs light with a certain wavelength [41,42].

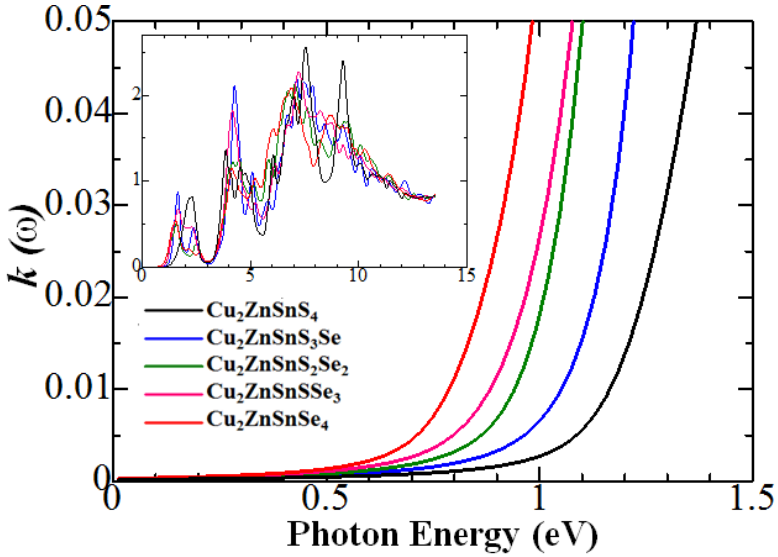

Figure 5 Dependences of the extinction coefficient of nanocrystals of the $Cu_2ZnSn[S_{1-x}Se_x]_4$ family on the photon energy (inset: k(ω) in the range from 0 to 14 eV).

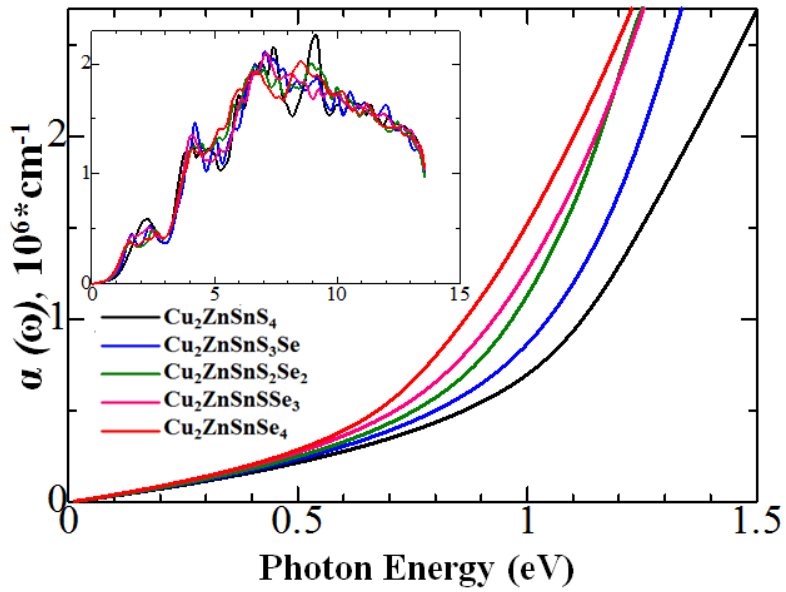

Figure 6 Dependences of the absorption coefficient on the photon energy for the model structures of the $Cu_2ZnSn[S_{1-x}Se_x]_4$ system (inset: α(ω) in the range from 0 to 14 eV).

The absorption coefficient (α) is one of the most important parameters for materials used as absorbing layers in photovoltaic cells. The maximum absorption of the studied materials is in the ultraviolet region. On the other hand, absorption coefficient shows the depth of penetration of light of a certain wavelength before absorption and depends on both the incident light and the internal properties of the material [43,44]. The rate of absorption of light is proportional to the intensity (the flux of photons) for a given wavelength. That is, light that is transmitted through the absorbing material is attenuated by a significant amount as it passes through; in other words, as light passes through the material the flux of photons is diminished by the fact that some are absorbed on the way through. Therefore, the amount of photons that reach a certain point in the semiconductor depends on the wavelength of the photon and the distance from the surface. Typically, absorption is selective selective in nature, i.e. light of different wavelengths is absorbed differently. Since the wavelength determines the color of light, therefore, rays of different colors are absorbed differently in a given substance. A recent study shows that as the wavelength of light increases, there is a corresponding increase in penetration depth [45]. In this case, transparent bodies are bodies that give a small absorption of light of all wavelengths related to the interval of visible rays, and the dependence of α on λ is a curve with a number of maxima, which, in turn, are absorption bands of light by a substance for a certain wavelength interval. According to **Figure 6**, the absorptivity of the studied systems increases with an increase in the selenium concentration; therefore, for $Cu_2ZnSnSe_4$, maximum absorption is observed in the IR region and covers the maximum range of the solar spectrum. The maximum extinction and absorption coefficients are in the same energy range, which agrees with the dispersion theory [46].

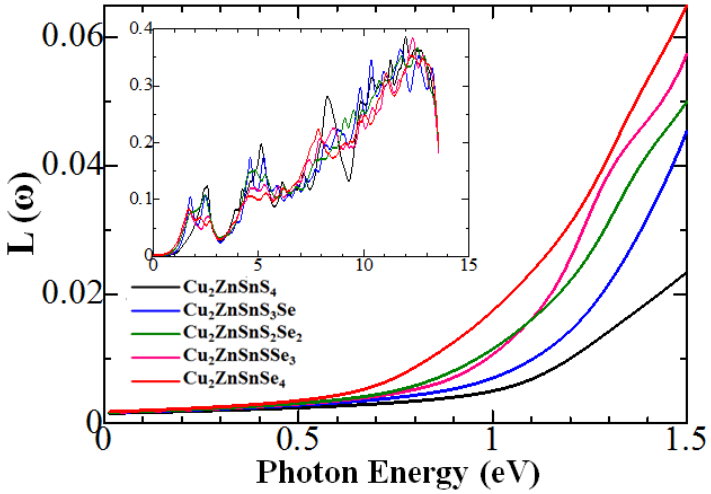

Figure 7 Calculated energy loss spectrum for the $Cu_2ZnSn[S_{1-x}Se_x]_4$ system depending on the energy (insert: L(ω) in the range from 0 to 14 eV).

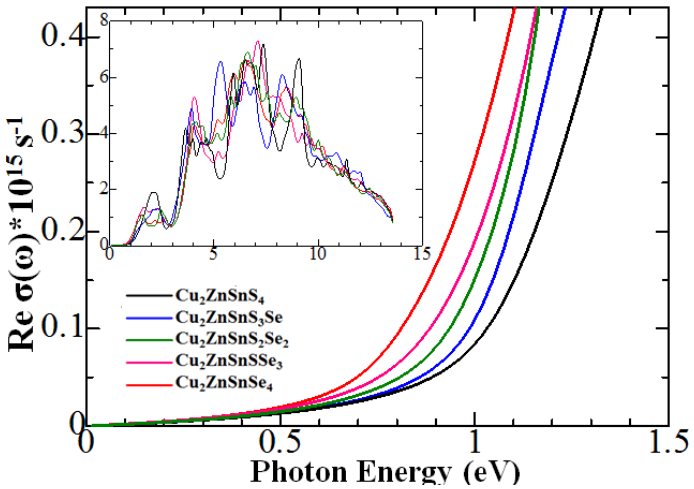

Figure 8 Spectra of the real part of the optical conductivity of the $Cu_2ZnSn[S_{1-x}Se_x]_4$ system as a function of energy (inset: σ(ω) in the range from 0 to 14 eV).

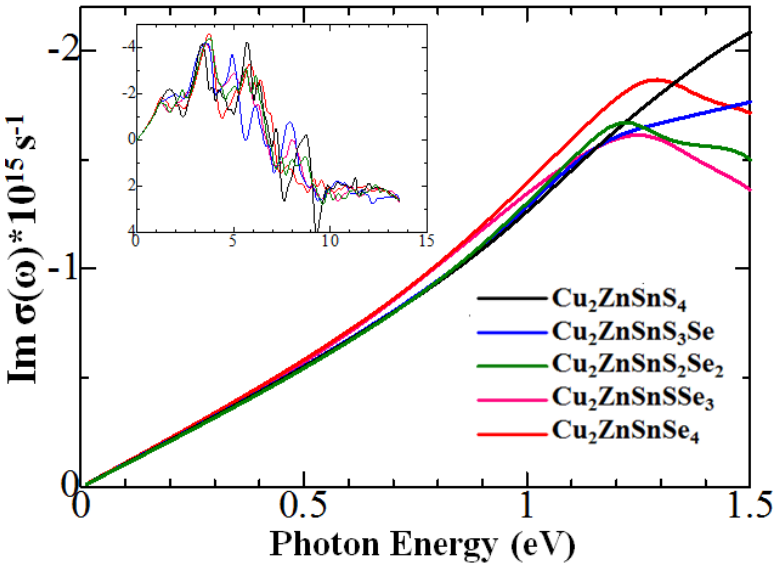

Figure 9 Spectra of the imaginary part of the optical conductivity of the $Cu_2ZnSn[S_{1-x}Se_x]_4$ system as a function of energy (inset: σ(ω) in the range from 0 to 14 eV).

The shape of the curves of the extinction coefficient k(ω) shown in **Figure 5** is in good agreement with the maxima of the imaginary part of the permittivity $\varepsilon_2(\omega)$. Calculations of the absorption coefficient show that, as always, the absorption maximum is in the ultraviolet region. For solar cells, the energy range of visible and IR light is important, where the average order of magnitude of α exceeds 10^4 cm^{-1}, while the materials under study have a higher absorption coefficient, which is remarkably suitable for absorbing layers of thin-film solar cells. This result agrees with the values obtained in experiments [47]. It can be seen from the obtained results that with an increase in the selenium concentration in the system, the absorption in this region increases, which is associated with a larger imaginary part of the dielectric function $\varepsilon_2(\omega)$ of Cu_2ZnSnS_4 compared to $Cu_2ZnSnSe_4$. In the region of intrinsic absorption, the absorption edge of Cu_2ZnSnS_4 is shifted to the blue region compared to the absorption edge of $Cu_2ZnSnSe_4$, in accordance with a slightly larger band gap. The calculated values of the optical band gap obtained using the Kubelka - Munk functions ($(\alpha h\nu)^{1/2}$, where α is the absorption coefficient) depending on the photon energy (hν), also confirmed the decrease in the band gap of the $Cu_2ZnSn[S_{1-x}Se_x]_4$ system with increasing selenium content. The optical band gap in our calculations decreases from 1.3 to 0.95 eV with the gradual replacement of Se by S, these values are consistent with the electronic band gaps recorded in them of about 1.0 eV for $Cu_2ZnSnSe_4$ and 1.44 eV for Cu_2ZnSnS_4 [48,49]. **Table 2** shows the calculated average values of the static (ε_0) and high-frequency (ε_∞) permittivity for the materials under study and compared with the literature data.

Table 2 Comparison of the results of calculations of ε_0 and ε_∞ with literature data.

$Cu_2ZnSn[S_{1-x}Se_x]_4$	ε_0		ε_∞	
	This work	In literature	This work	In literature
x = 0.00	9.83	10.4[e], 8.24[f]	8.30	7.9[e]
x = 0.25	9.52	9.5[e], 7.89[f]	7.50	7.5[e]
x = 0.50	9.35	9.4[e], 7.51[f]	7.21	7.2[e]
x = 0.75	9.11	9.2[e], 7.28[f]	6.73	6.8[e]
x = 1.00	8.67	9.0[e], 6.75[f]	6.52	6.5[e]

[e][50] and [f][51]

According to **Table 2**, our results are somewhat lower than those obtained by the HSE06 method in [50], however, all obtained values of ε_0 are larger than the results given in [51]. It can be seen that the calculated permittivities decrease when selenium is replaced with sulfur, which indicates an inverse relationship between the energy gap and the dielectric response. As shown in **Figure 2**, starting from a photon energy of 10 eV, the real part of the permittivity approaches 0, which means that the optical reflection coefficient R(ω) drops sharply, which is consistent with the results of our previous calculations on the study of the reflectivity of these nanocrystals. Thus, the S/Se ratio can be used to adjust the optimal band gap of the $Cu_2ZnSn[S_{1-x}Se_x]_4$ system.

Conclusions

In this work, the optical properties of the $Cu_2ZnSn[S_{1-x}Se_x]_4$ system on the basis of first-principles calculations using the mBJ exchange-correlation potential were studied. The main results obtained indicate that the absorption of solar radiation by these materials when used in solar cells is associated with electronic transitions from the antibonding states of Cu-3d/S-3p to the antibonding states of Sn-5s/S-3p. According to the results, the permittivity curves and the main optical spectra of all members of the $Cu_2ZnSn[S_{1-x}Se_x]_4$ family have fairly similar features in the IR region ofн radiation, despite the different composition and structure. It was found that the optical absorption coefficient, which is proportional to the imaginary part of the permittivity, is quite large in the IR and visible light energy range ($> 10^4$ cm^{-1}). It became known that all nanocrystals of the $Cu_2ZnSn[S_{1-x}Se_x]_4$ system are transparent in the high-energy region, which does not affect the absorption of visible light. In accordance with the above properties, Se-doped Cu_2ZnSnS_4 kesterites are promising materials for use as an absorber in thin-film solar cells.

Acknowledgements

The work was carried out as part of an internship for young researchers from the CIS countries, organized with the direct support of the Interstate Fund for Humanitarian Cooperation of the CIS Member States at the CIS International Center for Nanotechnology and the JINR laboratory. The authors express their gratitude to the management of the International Fund for Humanitarian Cooperation of the CIS Member States and the International Innovation Center for Nanotechnologies of the CIS for organizing and conducting internships for young scientists in the city of Dubna and the JINR laboratories.

References

[1] PCK Vesborg and TF Jaramillo. Addressing the terawatt challenge: Scalability in the supply of chemical elements for renewable energy. *RSC Adv.* 2012; **2**, 7933-47.
[2] M Jiang and X Yan. *Cu_2ZnSnS_4 thin film solar cells: Present status and future prospects. In*: A Morales-Acevedo [Ed.]. Solar Cells. IntechOpen, USA, 2013, p. 107-43.
[3] MA Green, K Emery, Y Hishikawa, W Warta and ED Dunlop. Solar cell efficiency tables (version 42). *Progr. Photovoltaics Res. Appl.* 2013; **18**, 144-50.
[4] MA Green, K Emery, Y Hishikawa and W Warta. Solar cell efficiency tables (version 35*). Progr. Photovoltaics Res. Appl.* 2013; **21**, 827-37.
[5] C Candelise, JF Speirs and RJ Gross. Materials availability for thin film (TF) PV technologies development: A real concern. *Renew. Sustain. Energ. Rev.* 2021; **15**, 4972-81.
[6] A Feltrin and A Freundlich. Material considerations for terawatt level deployment of photovoltaics. *Renew. Energ.* 2018; **33**, 180-5.
[7] V Fthenakis. Sustainability of photovoltaics: The case for thin-film solar. *Renew. Sustain. Energ. Rev.* 2009; **13**, 2746-50.
[8] MA Green. Consolidation of thin film photovoltaic technology: The coming decade of opportunity. *Progr. Photovoltaics Res. Appl.* 2006; **14**, 383-92.
[9] MA Green. Estimates of Te and In prices from direct mining of known ores. *Progress in Progr. Photovoltaics Res. Appl.* 2019; **17**, 347-59.
[10] CS Tao, J Jiang and M Tao. Natural resource limitations to terawatt-scale solar. *Sol. Energ. Mater. Sol. Cell.* 2021; **95**, 3176-80.
[11] C Wadia, AP Alivisatos and DM Kammen. Materials availability expands the opportunity for large-scale photovoltaics deployment. *Environ. Sci. Tech.* 2019; **43**, 2072-7.
[12] A Zuser and H Rechberger. Considerations of resource availability in technology development strategies: The case study of photovoltaics. *Resour. Conservat. Recycl.* 2021; **56**, 56-65.

[13] T Wu, Z Qin, Y Wang, Y Wu, W Chen, S Zhang, M Cai, S Dai, J Zhang, J Liu, Z Zhou, X Liu, H Segawa, H Tan, Q Tang, J Fang, Y Li, L Ding, Z Ning, …, L Han. The main progress of perovskite solar cells in 2020 - 2021. *Nano-Micro Lett.* 2021; **13**, 152.

[14] S Shauddin. Comparison among various emerging PV Cells with history, current status and future challenges. *Energ. Power* 2013; **3**, 91-105.

[15] S Bag, O Gunawan, T Gokmen, Y Zhu, TK Todorov and DB Mitzi. Low band gap liquid-processed CZTSe solar cell with 10.1 % efficiency. *Energ. Environ. Sci.* 2012; **5**, 7060-5.

[16] J Han, Y Zhou, Y Tian, Z Huang, X Wang, J Zhong, Z Xia, B Yang, H Song and J Tang. Hydrazine processed Cu_2SnS_3 thin film and their application for photovoltaic devices. *Front. Optoelectronics* 2014; **7**, 37-45.

[17] I Repins, C Beall, N Vora, C DeHart, D Kuciauskas, P Dippo, B To, J Mann, WC Hsu, A Goodrich and R Noufi. Co-evaporated $Cu_2ZnSnSe_4$ films and devices. *Sol. Energ. Mater. Sol. Cell.* 2022; **101**, 154-9.

[18] D Tiwari, TK Chaudhuri, T Shripathi, U Deshpande and V Sathe. Structural and optical properties of layer-by-layer solution deposited Cu_2SnS_3 films. *J. Mater. Sci. Mater. Electron.* 2014; **25**, 3687-94.

[19] WebElements. The periodic table of the elements, Available at: http://www.webelements.com, accessed March 2022.

[20] W Shockley and HJ Queisser. Detailed balance limit of efficiency of *p-n* junction solar cells. *J. Appl. Phys.* 1961; **32**, 510.

[21] T Kato, H Hiroi, N Sakai and H Sugimoto. Buffer/absorber interface study on Cu_2ZnSnS_4 and $Cu_2ZnSnSe_4$ based solar cells: Band alignment and its impact on the solar cell performance. *In*: Proceedings of the 28th European Photovoltaic Solar Energy Conference, Villepinte, France. 2013, p. 2125-7.

[22] M Nakashima, J Fujimoto, T Yamaguchi and M Izaki. Cu_2SnS_3 thin-film solar cells fabricated by sulfurization from NaF/Cu/Sn stacked precursor. *Appl. Phys. Express* 2015; **8**, 042303.

[23] VA Belyakov, VA Burdov, R Lockwood and A Meldrum. Silicon nanocrystals: Fundamental theory and implications for stimulated emission (*in Russian*). *Adv. Opt. Tech.* 2018; **279**, 502-9.

[24] P Hohenberg and W Kohn. Inhomogeneous electron gas. *Phys. Rev.* 1964; **136**, B864-B871.

[25] W Kohn and LJ Sham. Self-consistent equations including exchange and correlation effects. *Phys. Rev.* 1965; **140**, A1133-A1138.

[26] K Schwarz, P Blaha and GKH Madsen. Electronic structure calculations of solids using the WIEN2k package for material science. *Comput. Phys. Comm.* 2002; **147**, 71-6.

[27] DD Nematov, KT Kholmurodov, S Aliona, K Faizulloev, V Gnatovskaya and T Kudzoev. A DFT study of structure, electronic and optical properties of Se-doped kesterite Cu_2ZnSnS_4 (CZTSSe). *Lett. Appl. Nanobiosci.* 2022; **12**, 67.

[28] D Koller, F Tran and P Blaha. Merits and limits of the modified Becke-Johnson exchange potential. *Phys. Rev. B* 2011; **83**, 195134.

[29] N KodanSushil, AS Auluck and BR Mehta. A DFT study of the electronic and optical properties of a photovoltaic absorber material Cu2ZnGeS4 using GGA and mBJ exchange correlation potentials. *J. Alloy. Comp.* 2016; **675**, 236-43.

[30] ND Davlatshoevich, KM Ashur, BA Saidali, KK Tagoykulovich, A Lyubchyk and M Ibrahim. Investigation of structural and optoelectronic properties of n-doped hexagonal phases of TiO_2 ($TiO_{2-x}N_x$) nanoparticles with DFT realization: Optimization of the band gap and optical properties for visible-light absorption and photovoltaic applications. *Biointerface Res. Appl. Chem.* 2022; **12**, 3836-48.

[31] AS Doroshkevich, AA Nabiev, AV Shylo, A Pawlukojć, VS Doroshkevich, VA Glazunova, TY Zelenyak, NV Doroshkevich, KR Rahmonov, EK Khamzin, DD Nematov, AS Burhonzoda, MA Khusenov, KT Kholmurodov, S Majumder, M Balasoiu, A Madadzada and VI Bodnarchuk. Frequency modulation of the Raman spectrum at the interface DNA - ZrO_2 nanoparticles. *Egypt. J. Chem* 2019; **62**, 13-20.

[32] DD Nematov. Influence of iodine doping on the structural and electronic properties of $CsSnBr_3$. *Int. J. Appl. Phys.* 2022; **7**, 36-47.

[33] DD Nematov, KT Kholmurodov, DA Yuldasheva, KR Rakhmonov and IT Khojakhonov. Ab-initio study of structural and electronic properties of perovskite nanocrystals of the $CsSn[Br_{1-x}I_x]_3$ family. *HighTech Innovat. J.* 2022; **3**, 140-50.

[34] DD Nematov. Investigation optical properties of the orthorhombic system $CsSnBr_{3-x}I_x$: Application for solar cells and optoelectronic devices. *J. Hum. Earth Future* 2021; **2**, 404-11.

[35] P Blaha, K Schwarz, F Tran, R Laskowski, GKH Madsen and LD Marks. WIEN2k: An APW+lo program for calculating the properties of solids. *J. Chem. Phys.* 2020; **152**, 74101.
[36] M Gajdoš, K Hummer, G Kresse, J Furthmüller and F Bechstedt. Linear optical properties in the projector-augmented wave methodology. *Phys. Rev. B* 2006; **73**, 045112.
[37] N Kattan, B Hou, DJ Fermín and D Cherns. Crystal structure and defects visualization of Cu_2ZnSnS_4 nanoparticles employing transmission electron microscopy and electron diffraction. *Appl. Mater. Today* 2015; **1**, 52-9.
[38] A Nagaoka, K Yoshino, H Taniguchi, T Taniyama, K Kakimoto and H Miyake. Growth and characterization of $Cu_2ZnSn(S_xSe_{1-x})_4$ alloys grown by the melting method. *J. Cryst. Growth* 2014; **386**, 204-7.
[39] J He, L Sun, N Ding, H Kong, S Zuo, S Chen, Y Chen, P Yang and J Chu. Optical and electrical properties study of sol-gel derived Cu_2ZnSnS_4 thin films for solar cells. *AIP Adv.* 2014; **4**, 097115.
[40] ID Olekseyuk, LD Gulay, IV Dydchak, LV Piskach, OV Parasyuk and OV Marchuk. Single crystal preparation and crystal structure of the $Cu_2Zn(Cd,Hg)SnSe_4$ compounds. *J. Alloy. Comp.* 2002; **340**, 141-5.
[41] K Yamada, S Funabiki, H Horimoto, T Matsui, T Okuda and S Ichiba. Structural phase transitions of the polymorphs of $CsSnI_3$ by means of rietveld analysis of the x-ray diffraction. *Chem. Lett.* 1991; **20**, 801-4.
[42] AM Abd-Elnaiem, AM Abdelraheem and MA Abdel-Rahim. Substituting silver for tellurium in selenium-tellurium thin films for improving the optical characteristics. *J. Inorg. Organomet. Polym.* 2022; **32**, 2009-21.
[43] M Zafar, MK Masood, M Rizwan, A Zia, S Ahmad, A Akram and M Shakil. Theoretical study of structural, electronic, optical and elastic properties of $Al_xGa_{1-x}P$. *Optik* 2017; **182**, 1176-85.
[44] M Zafar, M Shakil, S Ahmed and MA Choudhary. Ab initio study of structural, electronic and elastic properties of $CdSe_{1-x}S_x$ semiconductor. *Sol. Energ.* 2017; **158,** 63-70.
[45] C Ash, M Dubec, K Donne and T Bashford. Effect of wavelength and beam width on penetration in light-tissue interaction using computational methods. *Laser. Med. Sci.* 2017; **32**, 1909-18.
[46] L Yao, L Dai, L Zheng and Q Zhou. A review on partial-wave dynamics with chiral effective field theory and dispersion relation. *Rep. Progr. Phys*. 2021; **84**, 076201.
[47] K Wang, O Gunawan, T Todorov, B Shin, S Chey, N Bojarczuk, D Mitzi and S Guha. Thermally evaporated Cu_2ZnSnS_4 solar cells. *Appl. Phys. Lett.* 2010; **97**, 143508.
[48] S Chen, A Walsh, JH Yang, X G Gong, L Sun, PX Yang, JH Chu and SH Wei. Theoretical study on the kesterite solar cells based on $Cu_2ZnSn(S,Se)_4$ and related photovoltaic semiconductors. *Chin. Phys. Rev. B* 2011; **83**, 125201.
[49] H Matsushita, T Maeda, A Katsui and T Takizawa. Thermal analysis and synthesis from the melts of Cu-based quaternary compounds Cu-III-IV-VI_4 and Cu_2-II-IV-VI_4 (II=Zn, Cd; III=Ga, In; IV=Ge, Sn; VI=Se). *J. Cryst. Growth* 2000; **208**, 416-22.
[50] SY Li, S Zamulko, C Persson, N Ross, JK Larsen and C Platzer-Björkman. Optical properties of Cu_2ZnSn $(Se_xS_{1-x})_4$ solar absorbers: Spectroscopic ellipsometry and ab initio calculations. *Appl. Phys. Lett.* 2017; **110**, 021905.
[51] MI Ziane, H Bennacer, M Mostefaoui, M Tablaoui, M Hadjab, A Saim and K Bekhedda. Anisotropic optical properties of $Cu_2ZnSn(S_xSe_{1-x})_4$ solid solutions: First-principles calculations with TB-mBJ+U. *Optik* 2021; **243**, 167490.